

Research Article

Intraoral Film Containing Insulin-Phospholipid Microemulsion: Formulation and *In Vivo* Hypoglycemic Activity Study

Heni Rachmawati,^{1,2,4} Bernard Manuel Haryadi,¹ Kusnandar Anggadiredja,¹ and Veinardi Suendo^{2,3}

Received 5 June 2014; accepted 1 December 2014; published online 16 December 2014

Abstract. Non-invasive administration of insulin is expected for better diabetes mellitus therapy. In this report, we developed intraoral preparation for insulin. Insulin was encapsulated into nanocarrier using self-assembly emulsification process. To increase lipophilicity of insulin, it was dispersed in phospholipid resulted in insulin-phospholipid solid dispersion. The microemulsion formula was established from our previous work which contained glyceryl monooleate (GMO), Tween 20, and polyethylene glycol (PEG 400) in a ratio of 1:8:1. To confirm the formation of insulin-phospholipid solid dispersion, PXRD, FTIR spectroscopy, and Raman spectroscopy were performed. Then, the microemulsion was evaluated for droplet size and distribution, zeta potential, entrapment efficiency, physical stability, and Raman spectroscopy. In addition, microemulsion with expected characteristic was evaluated for *in vitro* release, *in vitro* permeation, and *in vivo* activity. The droplets size of ~100 nm with narrow distribution and positive charge of +0.56 mV were formed. The insulin encapsulated in the oil droplet was accounted of >90%. Water-soluble chitosan seems to be a promising film matrix polymer which also functioned as insulin release controller. Oral administration of insulin microemulsion to healthy Swiss-Webster mice showed hypoglycemic effect indicating the success of this protein against a harsh environment of the gastrointestinal tract. This effectiveness significantly increased by fourfold as compared to free insulin. Taken together, microemulsion seems to be a promising carrier for oral delivery of insulin.

KEY WORDS: diabetes mellitus; hypoglycemia; insulin; phospholipid; self-assembly microemulsion.

INTRODUCTION

Insulin injection remains as a standard therapy for patients with type I diabetes (1). However, this therapy has disadvantages such as low patient acceptance due to pain and bruise at the administration site, besides lack of control in blood glucose levels (2,3). Oral insulin is considered more beneficial for patients, not only because it can provide a similar pattern of insulin fate compared to the physiological fate but also it can provide better glucose homeostasis (4). However, insulin as a protein has some problems if given orally. Undergoing significant degradations of the protein in the gastrointestinal tract and poor absorption are the main crucial limitations (5–10). Development of an

appropriate delivery system for insulin, hence, is mandatory (11). An ideal strategy is in the encapsulated system which can improve protein stability and permeability as well as its release from the carrier upon reaching blood circulation.

Several carriers have been developed to improve the lack of properties of protein as a therapeutic agent. Some of them showed limitation such as toxicity issue of using organic solvents and process reproducibility when upscaled. Due to practical and safety reasons, nano- and/or microemulsion, in particular self assembly, process as a potential carrier for hydrophilic drugs such as proteins are more attracting, not only in parenteral but also in oral routes (12,13). Nanoemulsions consist of fine oil-in-water dispersions, having droplets covering the size range of 100–600 nm and kinetically stable. Unlike nanoemulsion, microemulsion is homogeneous, transparent, thermodynamically stable dispersions of water and oil, stabilized by a surfactant, usually in combination with a co-surfactant (13–15). In those size ranges, the carrier will be able to give better penetration through enterocytes (11). Other advantages are easy to manufacture and scale up and having wide applications in colloidal drug delivery systems for the purpose of drug targeting and controlled release. Microemulsion as a potential carrier has been demonstrated for several macromolecules such as calcitonin (16), peptide, and transforming growth factor alpha (17).

Three common microemulsion systems that have been widely studied were W/O (18,19), O/W (13,20,21), and W/O/W type (12,16). In general, there is a limitation to develop the W/O

Electronic supplementary material The online version of this article (doi:10.1208/s12249-014-0258-9) contains supplementary material, which is available to authorized users.

¹ School of Pharmacy, Bandung Institute of Technology, Ganesha 10, Bandung, 40132, Indonesia.

² Division of Nanomedicine, National Research Center for Nanotechnology, Bandung Institute of Technology, Ganesha 10, Bandung, 40132, Indonesia.

³ Department of Chemistry, Faculty of Mathematics and Natural Sciences, Bandung Institute of Technology, Ganesha 10, Bandung, 40132, Indonesia.

⁴ To whom correspondence should be addressed. (e-mail: hrachma@yahoo.comhrachma@yahoo.comhrachma@yahoo.com)

emulsion due to low patient acceptance and the risk of phase inversion problem when the emulsion contacts with the gastrointestinal tract. These are some of the disadvantages of the system. Using the W/O/W type, phase inversion can be reduced, although release from the double emulsion still can occur quickly. The present report described the oral self-assembly microemulsion with the O/W system for insulin using a similar system we developed previously for BSA (22). Prior to emulsification process, insulin was incorporated into oil phase. To improve the oil miscibility of insulin, it was dispersed in phospholipid matrix. The main aim of incorporating the protein in oil phase was not only to improve protein permeability but also to protect the direct contact of the protein during process and when entering a harsh aqueous environment of the gastrointestinal tract. Further, the established insulin microemulsion was incorporated into film matrix consisting of polymer and plasticizer to produce intraoral film, the final dosage form. Several analyses were performed to evaluate the physical characteristic of insulin microemulsion, *in vitro* release profile of insulin from matrix film, and the potential of insulin to reduce blood glucose level after oral administration to male healthy mouse. As comparison, same procedure was applied for free insulin given through oral and subcutaneous routes.

MATERIALS AND METHODS

Materials

Human recombinant insulin was from Sigma Aldrich (Singapore); soy phosphatidylcholine (phospholipid; Lipoid® S100) was kindly gifted from PT. Dankos Farma; glyceryl monooleate (GMO; Peceol®) was from PT. Tritunggal Artha Makmur (Indonesia); Tween 20, PEG 400, trichloroacetate (TCA), and KBr were from Merck (Indonesia); and water-soluble carboxymethyl chitosan (CMCs) was from Eastar Holding Group (China), Bradford reagent from Biorad (USA), and propylene glycol (PG) from PT. Brataco (Indonesia). *Python reticulatus* snake shed from Tamansari Zoo Bandung (Indonesia). Other reagents were analytical grade and were used without further purification.

Methods

Preparation of Self-assembly Insulin Microemulsion

Prior to emulsification process, solid dispersion of insulin-phospholipid (ratio of 1:2 and 1:20 *w/w*) was prepared. To study the influence of pH on the formation of insulin-phospholipid solid dispersion, various buffers (PBS, citrate buffer pH 2.7, glycine buffer pH 2.7, acetate buffer pH 4.5 and acetate buffer

pH 5.4) were used to dissolve both substances resulting in a final insulin concentration of 100 mg/mL. Then, insulin-phospholipid solution was freeze-dried (Christ® Alpha 2-4 LSC) under a pressure of 10 Pa for 48 h. Subsequently, various amounts of dried solid dispersion (Table I) were incorporated into oil phase containing glycerol monooleate/Tween 20/polyethylene glycol (1:8:1). Spontaneous oil droplets were formed immediately after water was added to the oil phase in the ratio of oil to water phase of 1:4 *w/v* under mild stirring of 100 rpm for 2 min. Freshly prepared insulin microemulsion was kept at room temperature and ready for further characterizations and evaluations. Validation process on the formulation was shortly performed to ensure the reproducibility of product characteristics including size and size distribution, zeta potential, protein content, and entrapment efficiency.

Physical Characterization of Insulin Microemulsion

Droplets Size, Size Distribution, and Zeta Potential. Droplet size, size distribution, and zeta potential were measured from the same sample. One part of microemulsion was mixed with four parts of deionized water and then stirred at 100 rpm for 15 min. The size and size distribution of microemulsion were measured using photon correlation spectroscopy as previously reported (23). Zeta potential value was measured using electrophoretic light scattering (Delsa™ Nano C Particle Analyzer, Beckman Coulter).

Entrapment Efficiency. Determination of entrapment efficiency was done using an indirect method by measuring free or untrapped protein in the external phase of microemulsion. To do so, one part of insulin microemulsion was admixed into four parts of 2% of TCA solution. Then, centrifugation at 12,000 rpm for 5 min was applied to collect the precipitate protein. The precipitate was washed with 2% TCA solution three times, each with 100 µL and further dissolved in 1 mL of deionized water. Forty milliliters of protein solution was mixed with 2 mL of Bradford reagent, incubated for 5 min to complete the reaction. Absorbance was measured using visible spectrophotometer (Beckman®DU 650i) at λ_{\max} 595 nm. The absorbance represents the amount of free protein or untrapped protein.

The percentage of entrapment efficiency was determined using following equation:

$$\text{Entrapment efficiency \%} = \frac{\text{added protein into SNE} - \text{free protein}}{\text{added protein into SNE}} \times 100\%$$

Physical Stability Test. Physical stability test on selected insulin microemulsion (using insulin solid dispersion at

Table I. The Influence of Insulin-Phospholipid Ratio on the Microemulsion Characteristics

Buffer system	Insulin/phospholipid ratio (<i>w/w</i>)	Droplet size of insulin microemulsion (nm)	Polydispersibility index	Entrapment efficiency (%)
pH 7.4 PBS	1:2	1755.60±123.65	0.428±0.171	78.30±5.20
	1:10	546.70±14.71	0.259±0.171	81.58±2.51
	1:20	328.00±34.05	0.269±0.019	84.01±1.97
pH 2.7 citrate buffer	1:2	1819.47±182.80	0.817±0.048	80.70±3.20
	1:10	227.93±19.13	0.179±0.027	86.91±2.12
	1:20	102.17±5.50	0.197±0.015	90.33±0.65

ratio of 1:2 and 1:20 *w/w*) was done by centrifugation at 14,000g for 20 min using Thermo Scientific® Sorvall™ ST16R, and the precipitate was further analyzed for Raman spectrograph.

Powder X-ray Diffractometry. X-ray diffraction analysis was performed using a powder X-ray diffractometer (Bruker AXS® D8 Advance™). Samples of 30–50 mg (pure insulin, pure phospholipid, physical mixture, and insulin-phospholipid solid dispersion at a ratio of 1:2 and 1:20 *w/w*) was placed in a sample container at 25°C, CuK α radiation ($K\alpha_1=1.54060$; $K\alpha_2=1.54439$), Ni filter, 40-kV voltage, and 35 mA. Diffractogram was measured at 3–50° 2theta range (2θ) using 0.02° step size at a 0.1-s/step scanning speed.

FTIR Spectroscopy. Sample preparation was carried out by KBr disc method, with the ratio of sample/KBr=1:100 *w/w*. Measurement was performed on same samples for powder X-ray diffractometry (PXRD) analysis

at a 4000–400- cm^{-1} range with 1- cm^{-1} resolution using Fourier transform infrared spectrophotometer (Jasco® 4200 series).

Raman Spectroscopy. Samples of 5–20 mg were placed on a spotting plate. The samples were analyzed using a 785-nm HeNe laser excitation (red laser) with an intensity of 50 mW and integration time of 90 s aimed directly at the sample using Bruker AXS® Senterra™. Scanning was performed at 3500–59 cm^{-1} with a resolution of 0.5 cm^{-1} .

In Vitro Release Test

In vitro release study was performed using vertical diffusion cells with an effective diffusion area of 1 cm^2 with the receptor medium of 5-mL simulated gastric fluid (SGF according to USP 32 without pepsin) or simulated intestinal

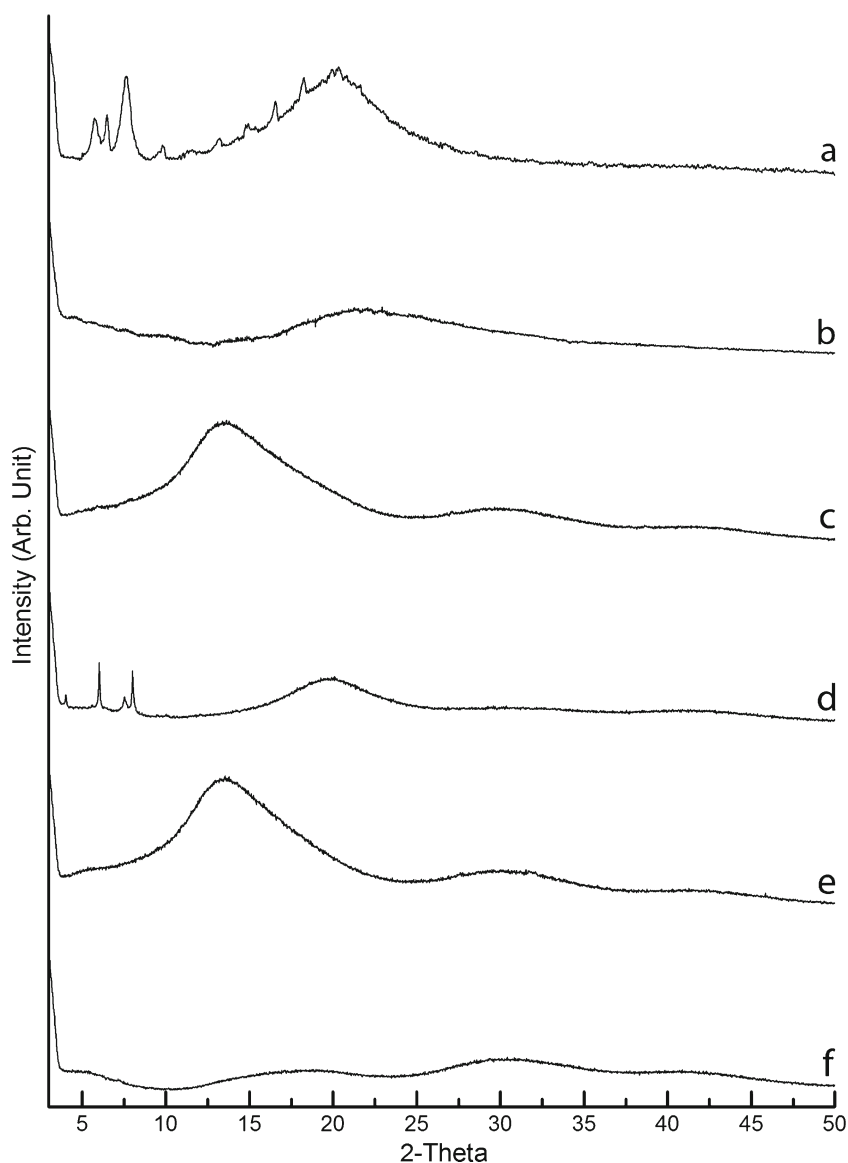


Fig. 1. X-ray diffractograms of **a** phospholipid, **b** insulin, **c** insulin-phospholipid physical mixture (1:2), **d** insulin-phospholipid solid dispersion (1:2), **e** insulin-phospholipid physical mixture (1:20), and **f** insulin-phospholipid solid dispersion (1:20)

Table II. Percentage of Crystallinity Amorphous from Tested Substances

Substances	Crystallinity (%)	Amorphicity (%)
Pure insulin	42.3	57.7
Insulin-phospholipid physical mixture PM (1:2)	57.6	42.4
Insulin-phospholipid solid dispersion (1:2)	36.1	63.9
Insulin-phospholipid physical mixture PM (1:2)	61.0	39.0
Insulin-phospholipid solid dispersion (1:20)	22.0	78.0

fluid (SIF according to USP 32 without pancreatin), agitation speed at 100 rpm and temperature kept at $37 \pm 0.5^\circ\text{C}$. Low protein adsorption membrane (Durapore® membrane, Millipore) was placed between the donor and receptor compartments. *In vitro* release study was conducted on insulin microemulsion, matrix film containing insulin (FLI), and matrix film containing insulin microemulsion (FLIN). Aliquots of 0.8 mL were taken at predetermined

time points, respectively, from SGF and SIF medium (0, 5, 10; 15, 20; 30, 45 min and 1, 1.5, 2) and (0, 5, 10; 15, 20; 30, 45 min and 1, 1.5, 2, 2.5, 3, 4, 5, 6, 8, 12, 24 h). An equal volume of fresh receptor medium was added to keep the volume constant. Subsequently, protein content in the aliquots was analyzed using micro-Bradford, and the absorbance was measured at λ_{max} of 595 nm. Blank microemulsion was used as a correction factor. Measurements were done as triplicate.

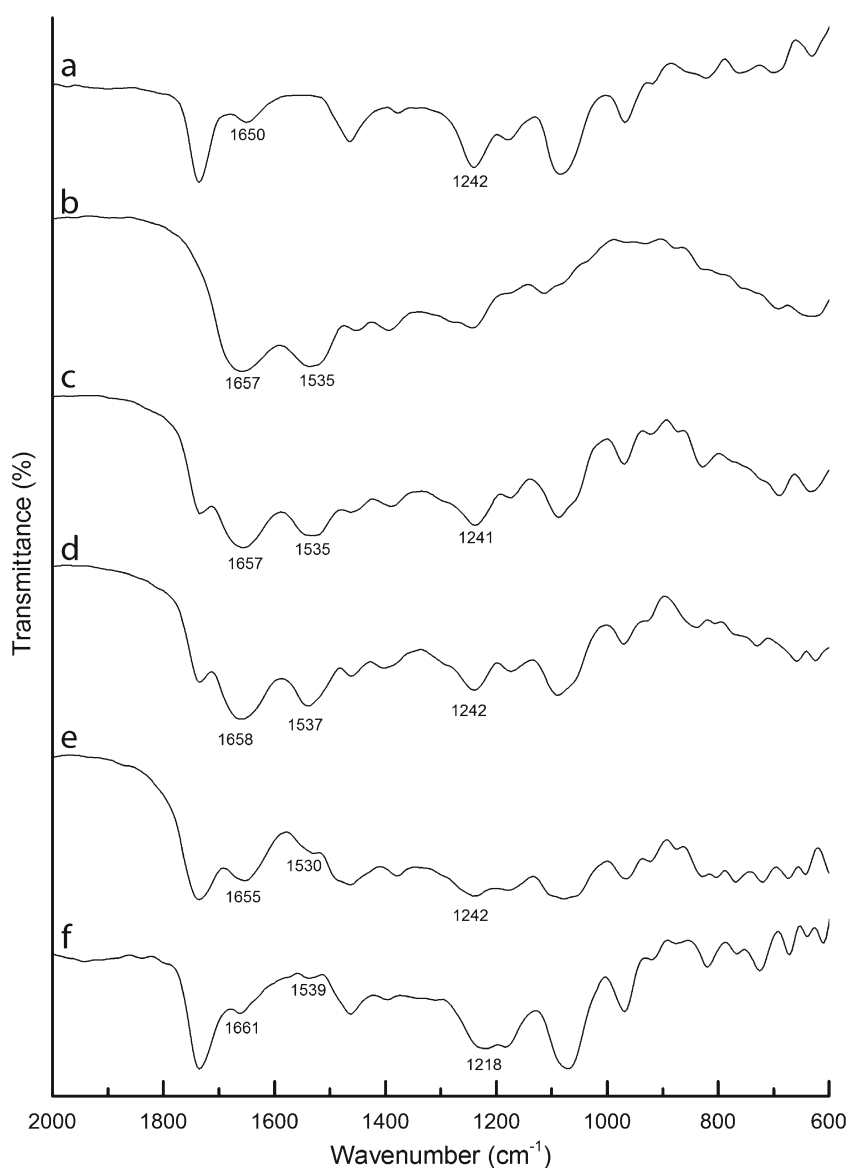


Fig. 2. FTIR spectra of **a** phospholipid, **b** insulin, **c** insulin-phospholipid physical mixture (1:2), **d** insulin-phospholipid solid dispersion (1:2), **e** insulin-phospholipid physical mixture (1:20), and **f** insulin-phospholipid solid dispersion (1:20)

Preparation of Intraoral Film Containing Insulin Microemulsion

Insulin microemulsion was incorporated into film matrix polymer containing 8% of water-soluble chitosan and 0.1% of propylene glycol as plasticizer, with a ratio of microemulsion/matrix polymer of 24%:76%. The evaluation of film forming matrix gel containing insulin microemulsion was including *in vitro* permeation and hypoglycemic activity studies.

In Vitro Permeation Study. *In vitro* permeation test was done through *P. reticulatus* snake shed. Prior to the test, the snake shed was soaked for 20 min and then rinsed three times with PBS pH 7.4 in order to minimize protein impurities. *In vitro* permeation test was performed for insulin microemulsion, insulin microemulsion in the film matrix (FLIN) solution, and pure insulin in the matrix (FLI) solution. Insulin solution was used as a control. Each sample contained 180 μg of insulin. Protein across the membrane was measured using a micro-Bradford method at a λ_{max} of 595 nm.

In vivo Activity Study. Hypoglycemic effect of insulin from different preparations was evaluated in healthy female mice (8–10 weeks; body weight of 20–30 g). Animal handling was performed according to good laboratory practice. The protocol for animal experiments was approved by the Faculty of Medicine,

Maranatha University-Immanuel Hospital Ethical Committee number 110/KEP FK UKM-RSI/VI/2013, Bandung, Indonesia, and the study was carried out in accordance with principles of laboratory animal care and approved protocols.

The mice were fasted overnight before and during the test, but allowed for water access. The insulin dose either for oral and subcutaneous administration was referred to Cui *et al.*, Peng *et al.*, and Zhou *et al.* (24–26). Based on their report, we did orientation of the insulin doses for oral and subcutaneous routes to obtain the most appropriate insulin doses which showed hypoglycemic effect without causing animal death. The mice were randomly divided into ten groups ($n=5$): (a) PBS given subcutaneously, (b) blank microemulsion given subcutaneously, (c) blank microemulsion given orally, (d) pure insulin in PBS given subcutaneously with a dose of 1 IU/kg, (e) insulin-phospholipid solid dispersion in PBS given subcutaneously with a dose of 1 IU/kg, (f) insulin microemulsion given subcutaneously with a dose of 1 IU/kg, (g) film matrix solution containing insulin microemulsion s.c. 1 IU/kg, (h) pure insulin in PBS given orally with a dose of 20 IU/kg, (i) insulin microemulsion given orally with a dose of 20 IU/kg, and (j) film matrix solution containing insulin microemulsion given orally with a dose of 20 IU/kg. Groups (a) to (c) were as negative controls, group (d) was the standard group. Blood samples were taken from vein tail at predetermined time points (0, 0.5, 1, 1.5, 2, 3, 4, 5, 6, 8; 12; 24 h), and blood glucose levels were measured with a glucose assay kit Accu-chek® (Roche). Pharmacological

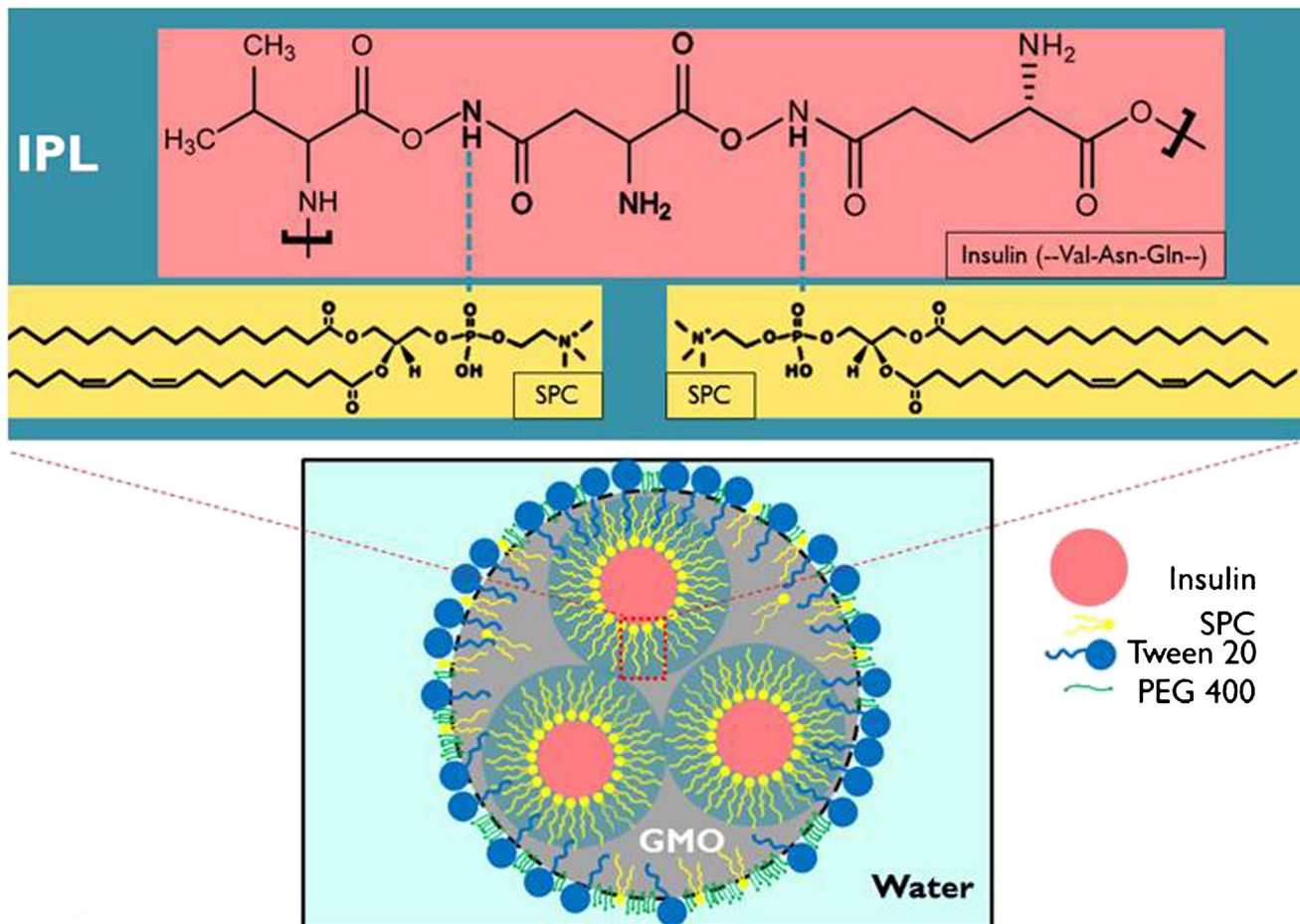


Fig. 3. Illustration of suggested interaction between insulin with phospholipid in insulin-phospholipid solid dispersion placed in microemulsion droplets. Insulin-phospholipid solid dispersion shows reverse micelle-like structure

availability, an observed parameter, at groups (e) to (j) was calculated using the following equations:

$$\text{Pharmacological Availability(\%)} = \frac{\text{AAC}_{(\text{formula})} \times \text{Dosis}_{(\text{standard})}}{\text{AAC}_{(\text{standard})} \times \text{Dosis}_{(\text{formula})}} \times 100\%$$

AAC is the area above the curve (the amount of blood glucose level reduction above the curve *versus* time).

Data Analysis

All data are expressed in average ± standard deviation (SD). Unless otherwise stated, all data obtained from triplicate (n=3). Statistical analysis used in this study was paired

t student, unpaired *t* student, and one-way ANOVA tests. Significant statistical differences were shown on the values of *P*<0.05.

RESULTS AND DISCUSSION

Powder X-ray Diffractometry

Powder X-ray diffractometry (PXRD) analysis was conducted to determine the changes of protein crystal structure in insulin solid dispersion. Figure 1 shows the diffractogram of pure phospholipid, pure insulin, physical mixture of insulin-phospholipid, and insulin-phospholipid solid dispersion. Pure phospholipid diffractogram shown in Fig. 1a has a sharp peak, and crystallinity occurs partially at 5 and 20°, which correlated with

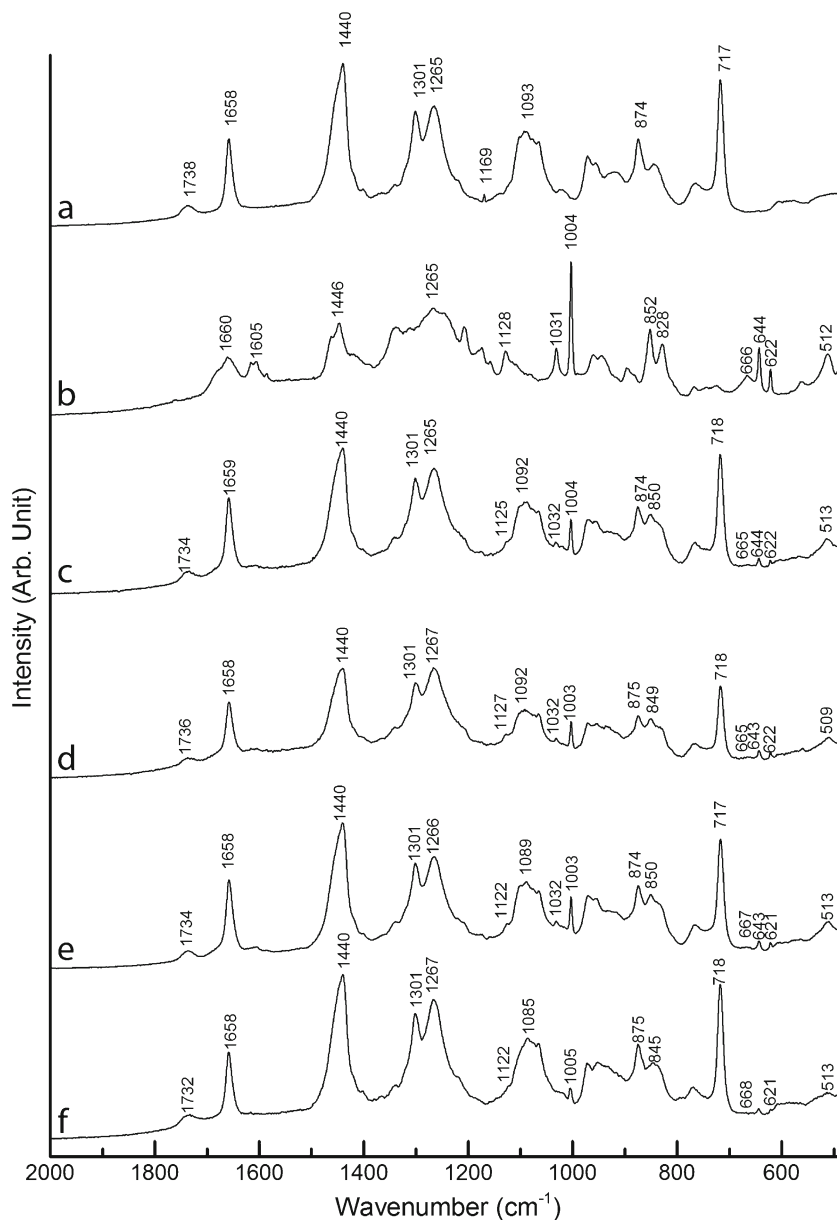


Fig. 4. Raman spectra of **a** phospholipid, **b** insulin, **c** insulin-phospholipid physical mixture (1:2), **d** insulin-phospholipid solid dispersion (1:2), **e** insulin-phospholipid physical mixture (1:20), and **f** insulin-phospholipid solid dispersion (1:20)

the data presented in Table II, while pure insulin diffractograms (1b) showed amorphous structure. As presented in Table II, all physical mixtures showed higher crystallinity than the solid dispersion. Insulin solid dispersion (1:20) diffractogram (Fig. 1d) showed high amorphous structure propensity, in contrast to 1:2 solid dispersion diffractogram (Fig. 1f) which appeared more crystalline when the crystallinity index was relatively higher than others. Amorphous diffractograms as shown in Fig. 1 indicated the molecular dispersion occurred between insulin and phospholipid (27). Separate crystallization is likely related to phosphate buffer (PBS) component which was not suitable as a cryoprotectant during freezing process. The early crystal formation was suggested coming from phosphate group. By changing the pH, either protein or phospholipid solubility was interfered. Premature crystallization of phosphate group from buffer solution was characterized by low T_g value (collapse temperature). This phenomenon did not appear when

solid dispersion was prepared in citrate buffer which resulted in good solid dispersion system. Citrate buffer has high T_g leading to low crystallization tendency, hence showing better cryoprotectant function. In addition, citrate buffer did not influence the protein activity and stability.

FTIR Spectroscopy

FTIR analysis was performed to study the interactions between insulin and phospholipid after solid dispersion protocol. FTIR spectra are presented in Fig. 2. Significant changes were observed as blueshift in the amide I region ($1650\text{--}1660\text{ cm}^{-1}$; ν (C = O)) and/or amide III region ($1530\text{--}1560\text{ cm}^{-1}$; δ (NH)) of the protein and also redshift in the phospholipid peak at 1242 cm^{-1} (ν P = O). These changes markedly occurred in solid dispersion with a higher content of phospholipid (1:20), in which the insulin peaks of 1657 and 1535 cm^{-1} were undergoing

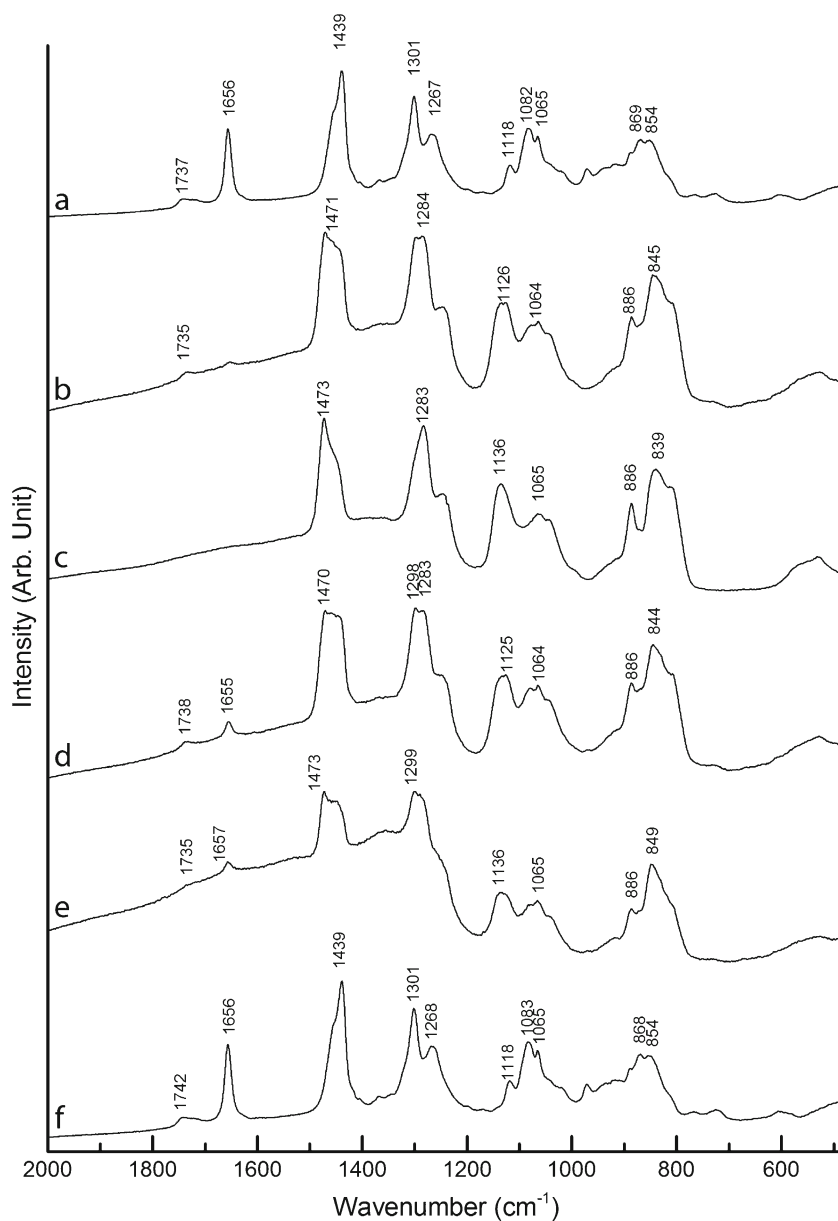


Fig. 5. Raman spectra of **a** GMO, **b** Tween 20, **c** PEG 400, **d** blank SNE, **e** blank microemulsion, and **f** phospholipid solution in GMO (1:5 w/w)

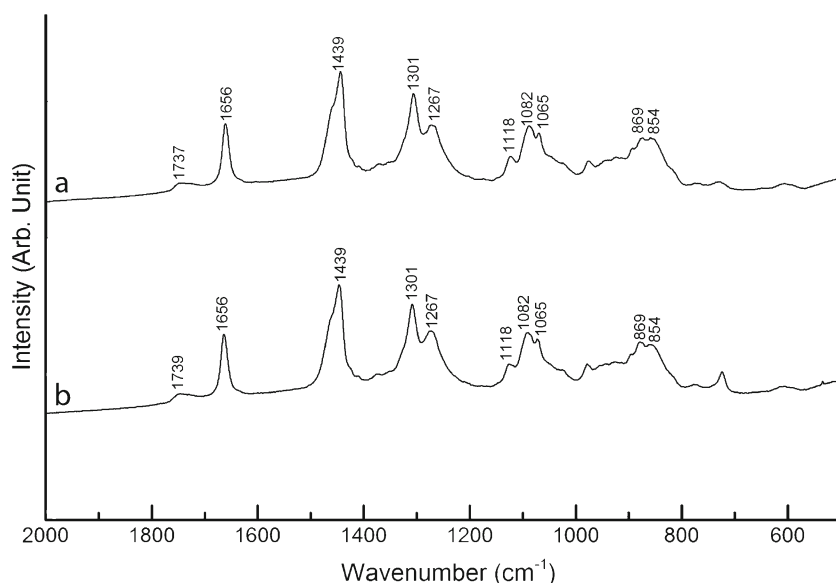


Fig. 6. Raman spectra of **a** insulin-phospholipid (IPL, 1:2) dispersion in GMO, **b** insulin-phospholipid (IPL, 1:20) dispersion in GMO

blueshift to 1661 and 1539 cm^{-1} , while phospholipid peak underwent redshift to 1218 cm^{-1} . At the amide I region, the shifting at a functional group of C = O occurred because of dissociation of intermolecular hydrogen bonds formed during lyophilization process.

Raman Spectroscopy

Raman analysis was performed to study the property of molecular structure (28) and to confirm the FTIR spectroscopic data. In this study, pellet and supernatant of formula (b)/insulin-phospholipid solid dispersion (1:2), oil phase components (GMO, Tween 20, PEG 400), and microemulsion were analyzed. The illustration of suggested interaction between insulin with phospholipid in insulin-phospholipid solid dispersion placed in microemulsion droplets is depicted in Fig. 3. Raman spectrographs of this structure, solid dispersion, and the all pure components of formula are shown in Figs. 4, 5, and 6.

Insulin showed peaks at 1660, 1605, 1446, 1265, 1128, 1031, 1004, 852, and 828 cm^{-1} (Fig. 4b). The insulin peaks could not be further identified when the solid dispersion was perfectly dispersed in GMO and similarly when the solid dispersion was encapsulated into oil droplets. Peak characteristics of microemulsion were in accordance with the peaks of GMO, Tween 20, and PEG 400 (Fig. 5a–c, respectively), with some shifts.

Table III. The Influence of Buffer System on the Droplet Size

Buffer system	Droplet size (nm)	Polydispersity index
PBS pH 7.4	1755.60±123.65	0.428±0.171
Citrate buffer pH 2.7	1819.47±182.80	0.455±0.029
Glycine buffer pH 2.7	2786.43±100.63	0.608±0.129
Acetate buffer pH 4.5	1654.03±116.56	0.803±0.052
Acetate buffer pH 5.4	1960.47±105.53	0.626±0.032
Deionized water	3413.90±654.60	0.817±0.105

Raman spectrum of pellets as shown in Fig. 6 indicated the presence of insulin-phospholipid solid dispersion in the external phase of the microemulsion. This means the loading capacity of the microemulsion formula was limited. Peak characteristic of pellet and insulin-phospholipid solid dispersion (1:2) was identical, *i.e.*, at 1003 cm^{-1} representing the presence of phenylalanine and tryptophan amino acids (29).

The solid dispersion between insulin and phospholipid was mediated through hydrophobic interaction of both compounds. The solid dispersion system and ratio of protein-phospholipid (*w/w*) influenced the successful formation of insulin-phospholipid solid dispersion, hence the insulin microemulsion (Tables I and III). As shown in Table I, different buffer systems (PBS pH 7.4, citrate buffer pH 2.7, glycine buffer pH 2.7, acetate buffer pH 4.5 and pH 5.4, and deionized water) produced microemulsion with different droplet sizes and size distributions. Citrate buffer produced a better performance of insulin microemulsion and used for further studies.

Table III shows the role of phospholipid to improve insulin lipophilicity which contributed to insulin entrapment efficiency in the oil droplets. In addition, the type of buffer in the insulin-phospholipid lyophilization was a very critical factor to maintain the compact structure of protein during freeze-drying process. Acidic environment was suggested to be the most appropriate condition for insulin to form better microemulsion. The concentration of insulin was also important to determine the

Table IV. The Influence of Insulin Amount on Droplets Size, Polydispersity Index, and Entrapment Efficiency

Amount of added insulin into 1-g SME (self microemulsion) (mg)	Parameter		
	Droplets size (nm)	Polydispersity index	Entrapment efficiency (%)
1	102.17±5.50	0.197±0.015	90.33±0.65
2	596.23±32.59	0.516±0.021	79.58±1.81
3	1202.40±41.07	0.750±0.037	66.43±2.31

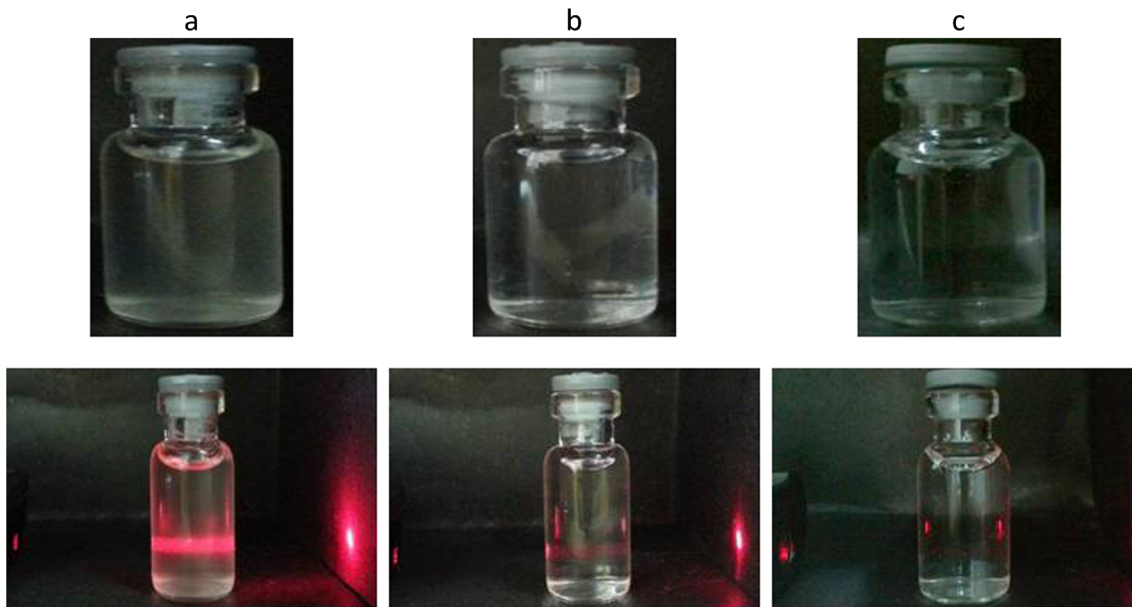


Fig. 7. Visual appearance (*above*) and observed Faraday-Tyndall effect (*below*) of **a** insulin-phospholipid solid dispersion (IPL, 1:2)—loaded microemulsion, **b** insulin-phospholipid solid dispersion (IPL, 1:20)—loaded microemulsion, and **c** deionized water

microemulsion characteristics (Table IV). To confirm the globule size of microemulsion, a simple observation was done with Faraday-Tyndall effect, and the result is presented in Fig. 7. As shown, light scattering effect was greater when the size of the

dispersed phase is larger (as in the case of formula (b)) resulting in a clearer conical light beam trajectory.

In Vitro Release Study

The *in vitro* release data through diffusion membrane is depicted in Fig. 8. As shown, it is clear that the presence of oil facilitated the diffusion of protein through the membrane. Unfortunately, the presence of chitosan as a film matrix delayed the diffusion rate of insulin, in particular to lower pH receiving medium. The swelling property of water-soluble chitosan when contacting with aqueous system enhanced the medium viscosity which further functioned as diffusion barrier for free or encapsulated insulin.

In Vitro Permeation

To confirm the release study using vertical diffusion cells, a model of biological membrane was performed. A model of mucosal membrane in intraoral cavity was ventral *P. reticulatus*

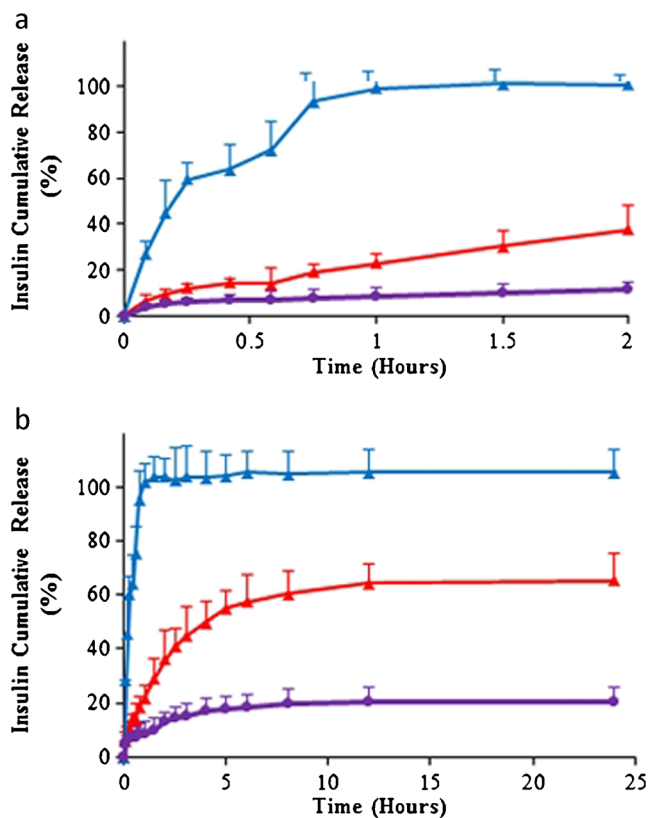


Fig. 8. *In vitro* insulin release profiles in **a** pH 1.2, **b** pH 6.8 of insulin microemulsion (—▲—), FLIM (—▲—), and FLI (—●—)

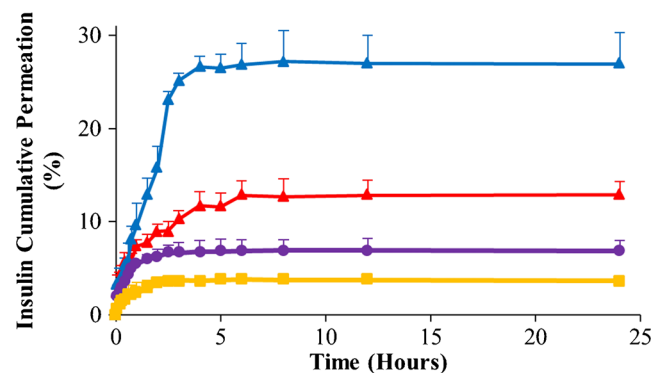


Fig. 9. *In vitro* insulin permeation profiles of insulin microemulsion (—▲—), FLIM (—▲—), FLI (—●—), and insulin solution (—■—)

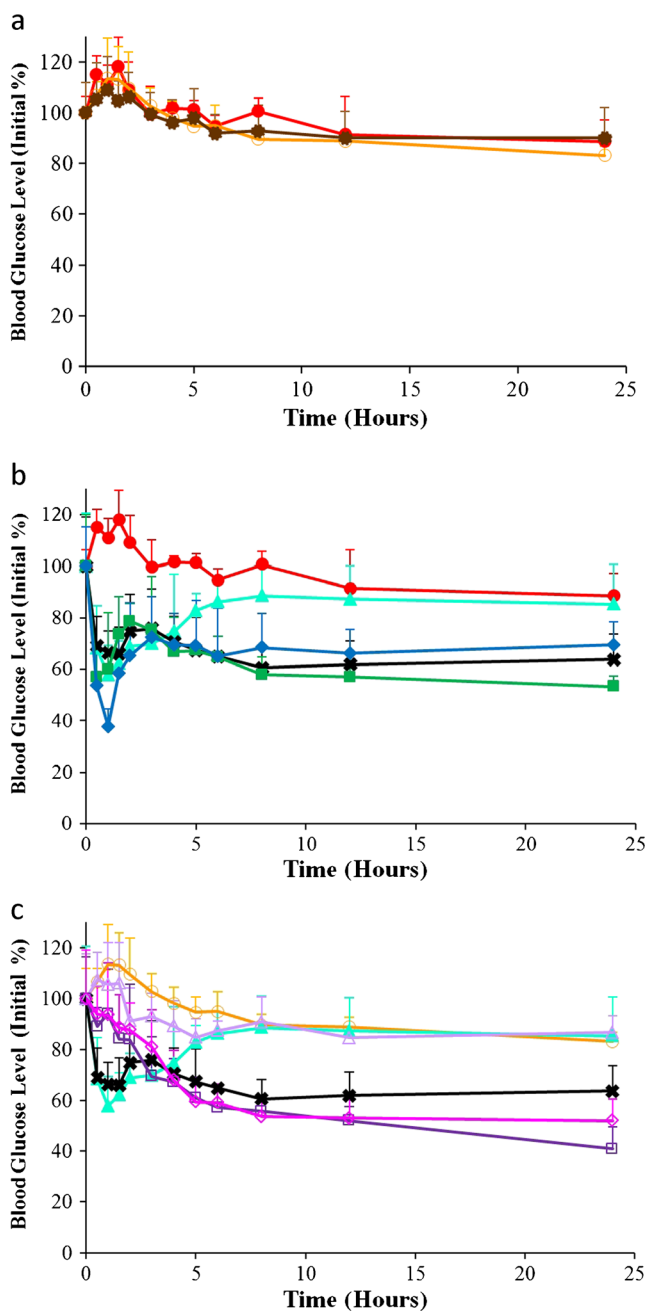


Fig. 10. a The curve of time vs. blood glucose profile of negative control preparations after being given to healthy mice: (—●—) blank microemulsion-subcutan, (—○—) blank microemulsion-oral, and (—■—) PBS-subcutan) ($n=5$ each group). b The curve of time vs. blood glucose profile of preparations after subcutaneous administration to healthy mice: (—●—) blank microemulsion, (—▲—) insulin solution dose of 1 IU/kg, (—■—) insulin-phospholipid solid dispersion dose of 1 IU/kg, (—■—) insulin microemulsion dose of 1 IU/kg, and (—◆—) film matrix containing insulin microemulsion dose of 1 IU/kg) ($n=5$ each group). c The curve of time vs. blood glucose profile of preparations after administration to healthy mice: (—▲—) insulin solution s.c. dose of 1 IU/kg, (—■—) insulin-phospholipid solid dispersion dose of 1 IU/kg, (—○—) blank microemulsion, oral), (—■—) insulin solution, oral dose of 20 IU/kg, (—■—) insulin microemulsion, oral dose of 20 IU/kg, and (—◆—) film matrix containing insulin microemulsion, oral dose of 20 IU/kg) ($n=5$ each group)

Table V. Pharmacological Availability Comparison from Various Preparations

Administration route and dose	Formula	Pharmacological availability (compared to insulin solution subcutaneous)
s.c.1 IU/kg	IPL dispersion	227.12
	Insulin NE	262.18
	FLIM	210.80
Oral 20 IU/kg	Insulin solution	3.41
	Insulin ME	14.62
	FLIM	13.33

IPL insulin phospholipid, FLIM matrix film containing insulin microemulsion

snake shed that is relatively difficult to be penetrated because of low permeability (30,31). In addition, soaked and rinsed snake shed practically did not release protein, hence more suitable for the permeability study of insulin.

The permeation data of insulin from various preparations is presented in Fig. 9. In line with the release study using vertical diffusion cells, encapsulated insulin in the oil droplet showed markedly enhanced permeability through the snake shed. Again, the presence of water-soluble chitosan retarded this property. Viscous polymer solution surrounding microemulsion obviously limited the movement of either microemulsion or the insulin released from the oil droplets.

In Vivo Activity

As there is a limitation to simulate intraoral situation for our insulin intraoral film preparation, the oral route was used to test hypoglycemic effect of insulin given through non-parenteral way. The activity study was conducted in healthy mouse. As a negative control of the formulas, blank microemulsion was given both subcutaneously and orally (Fig. 10a). As indicated, the blank microemulsion did not show any change in basal blood glucose level. In addition, to compare this non-parenteral route, subcutaneous injection of pure insulin was also performed. The hypoglycemic effect of pure insulin given subcutaneously is presented in Fig. 10b. As shown, the administration of pure insulin decreased the basal blood glucose level accounted as 60%, 1 h after administration and maintained for 5 h. Insulin-phospholipid solid dispersion was also tested to check insulin activity after being dispersed in phospholipid matrix. Indeed, there was activity reduction significantly as compared to pure insulin (Table V). From the time point of 6–12 h, there were significantly differences in the blood glucose levels between pure insulin versus insulin solid dispersion ($P<0.05$). The lower activity of insulin in solid dispersion system was clearly due to the presence of phospholipid matrix which delayed the release of insulin to enter blood circulation. The hydrophobic interaction between insulin and phospholipid as well as hydrophobic group of lipid structure in adipose tissue is suggested as the reason on this lower hypoglycemic effect.

Incorporation of insulin solid dispersion into oil droplet of microemulsion, however, improved the circulation time of insulin indicated by increased pharmacological activity up to 262.18%. The improved circulation time of insulin was clearly observed at 5–24 h after administration. This period is even expected in particular for diabetic patients to control blood glucose level at

a longer time. The presence of oil phase in the microemulsion as well as the lower size of the oil globule under nanometer range is suggested for permeation enhancement of insulin across biological membrane at the site of injection.

In contrast to *in vitro* permeation study, when insulin microemulsion was incorporated into film matrix consisting of water-soluble chitosan, the hypoglycemic effect of insulin after subcutaneous administration was improved as compared to insulin microemulsion itself. This is contradictory with the *in vitro* permeability study. The positive surface charge of chitosan generated by the acidic environment of the gastric tract seems to be important for its permeation enhancer function. The dual positive effects of hydrophilic environment from water-soluble chitosan and oil-based nanodroplets synergistically increased the insulin migration from the injection site into blood compartment.

The blood glucose level profile after oral administration of various insulin preparations is shown in Fig. 10c. As clearly shown, oral administration of pure insulin did not result in blood glucose level reduction at all, even after a 24-h observation. The failure of insulin to show the effect is well understood: proteolytic degradation and poor absorption. In contrast, insulin incorporated into oil globule of microemulsion showed pharmacological activity calculated as 14.62% (Table V). This means that microemulsion protected insulin from GIT degradation and improved the oral absorption. When the hypoglycemic effect of the same insulin preparation was compared between oral and subcutaneous administrations, significant difference of blood glucose level especially at 5–12 h was observed. This is also well understood. However, the most important point in this study is to show how our developed microemulsion and further intraoral formulation for insulin opens the opportunity for non-parenteral route. Although there was a different amount of insulin absorbed from microemulsion and microemulsion in the film matrix, the presence of hypoglycemic effect of insulin after oral administration of those two formulas indicated that there is no significant influence of chitosan on the fate of insulin microemulsion, then bioavailability.

CONCLUSION

Insulin, the most potent and durable hypoglycemic agent in an antidiabetic family, in some cases failed to achieve lasting blood glucose levels in diabetic patients. Non-physiological way of its administration with inappropriate pharmacodynamics is the main reason on this failure. Non-parenteral, either oral or intraoral, route has the potential of replacing preprandial insulin need and possible of serving a supplement to basal insulin. Microemulsion containing insulin encapsulated in the oil phase reported here seems to be a promising intermediate formulation strategy to make insulin given orally or intraorally. *In vitro* improvement of insulin permeation through diffusion membrane cell as well as snake shed which in turn gives better hypoglycemic effect are proof of this successful approach to protect insulin from presystemic degradation and to improve insulin absorption.

ACKNOWLEDGMENTS

This work was financially supported by a research grant from the Bandung Institute of Technology, Indonesia, 2013.

Conflict of Interest There is no conflict of interest to declare.

REFERENCES

- Triplitt CL, Reasner CA, Isle WL. Diabetes mellitus, 1205–1241 in book: pharmacotherapy: a pathophysiologic approach. 7th ed. New York: The McGraw-Hill Companies, Inc; 2008. p. 2597.
- Heineman L, Jacques Y. Oral insulin and buccal insulin: a critical reappraisal. *J Diabetes Sci Tech.* 2009;3(3):568–83.
- Heinemann L. New ways of insulin delivery. *Int J Clin Pract.* 2011;65:31–46.
- Lassmann-Vague V, Racca D. Alternatives routes of insulin delivery. *Diabetes Metab.* 2006;32:513–22.
- Rekha MR, Sharma CP. Oral delivery of therapeutic protein/peptide for diabetes—future perspectives. *Int J Pharm.* 2013;440:48–52.
- Pozzilli P, Raskin P, Parkin CG. Review of clinical trials: update on oral insulin spray formulation. *Diabetes Obes Metab.* 2010;12(2):1–8.
- Iyer H, Khedkar A, Verma M. Oral insulin—a review of current status. *Diabetes Obes Metab.* 2010;12(3):179–85.
- Ramesan RM, Sharma CP. Challenges and advances in nanoparticle-based oral insulin delivery. *Exp Rev Med Devices.* 2009;6(6):665–76.
- Khafagy ES, Morishita M, Onuki Y, Takayama K. Current challenges in non-invasive insulin delivery systems: a comparative review. *Adv Drug Del.* 2007;9:1521–46.
- Banga AK, editor. Therapeutic peptides and proteins formulation, processing, and delivery systems. 2nd ed. Boca Raton: Taylor & Francis; 2006. p. 14–83.
- Chen MC, Sonaje K, Chen KJ, Sung HW. A review of the prospects for polymeric nanoparticle platforms in oral insulin delivery. *Biomater.* 2011;32:9826–38.
- Li XY, Qi JP, Xie YC, Zhang X, Hu SW, Xu Y, *et al.* Microemulsions coated with alginate/chitosan as oral insulin delivery systems: preparation, characterization, and hypoglycemic effect in rats. *Int J Nanomedicine.* 2013;8:12–21.
- Rao SVR, Shao J. Self-microemulsion drug delivery systems (SNEDDS) for oral delivery of protein drugs 1: formulation development. *Int J Pharm.* 2008;362(2–3):7–8.
- Fryd MM, Mason TG. Advanced microemulsions. *Annu Rev Phys Chem.* 2012;6:493–518.
- Sattler V, Galindo-Alvarez JM, and Marie-Bégué E. Low energy emulsification methods for nanoparticles synthesis, 509–524 dalam Hashim, A.A. The delivery of nanoparticles. InTech, Rijeka-Croatia. 2012:p. 540.
- Dogru ST, Calis S, Oner F. Oral multiple W/O/W emulsion formulation of a peptide salmon calcitonin: in vitro-in vivo evaluation. *J Clin Pharm Ther.* 2000;25(6):435–43.
- Celebi N, Yetkin G, Ozer C, Can A, Gökçora N. Evaluation of microemulsion and liposomes as carriers for oral delivery of transforming growth factor alpha in rats. *J Microencapsul.* 2012;29(6):539–48.
- Çilek A, Çelebi N, Tirnaksiz F. Lecithin-based microemulsion of a peptide for oral administration: preparation, characterization, and physical stability of the formulation. *Drug Deliv.* 2005;13(1):19–24.
- Çilek A, Çelebi N, Tirnaksiz F, Tay A. A lecithin-based microemulsion of Rh-insulin with aprotinin for oral administration: investigation of hypoglycemic effects in non-diabetic and STZ-induced diabetic rats. *Int J Pharm.* 2006;298(1):176–85.
- Toorisaka E, Ono H, Arimori K, Kamiya N, Goto M. Hypoglycemic effect of surfactant-coated insulin solubilized in a novel solid-in-oil-in-oil water (S/O/W) emulsion. *Int J Pharm.* 2003;252:271–4.
- Morita T, Sakamura Y, Horikir Y, Suzuki T, Yoshino H. Protein encapsulation into biodegradable microspheres by a novel S/O/W emulsion method using poly(ethylene glycol) as a protein micronization adjuvant. *J Con Rel.* 2000;69:435–44.
- Rachmawati H, Haryadi DM. The influence of polymer structure on the physical characteristic of intraoral film containing BSA-loaded nanoemulsion. *J Nanomed Nanotechnol.* 2014;5(1):1–6.

23. Rachmawati H, Edityaningrum CA, Mauluddin R. Molecular inclusion complex of curcumin- β -cyclodextrin nanoparticle to enhance curcumin skin permeability from hydrophilic matrix gel. *Am Assoc Pharm Scie Pharm Sci Tech.* 2013;14(4):1303–12.
24. Cui FD, Shi K, Zhang LQ, Tao AJ, Kawashima Y. Biodegradable nanoparticles loaded with insulin-phospholipid complex for oral delivery: preparation, in vitro characterization and in vivo evaluation. *J Con Rel.* 2006;114:242–50.
25. Peng Q, Zhang ZR, Gong T, Chen GQ, Sun X. A rapid-acting, long-acting insulin formulation based on a phospholipid complex loaded PHBHHx nanoparticles. *Biomater.* 2012;33:1583–8.
26. Zhou CP, Xia XJ, Liu YL, Li L. The preparation of a complex of insulin-phospholipids and their interaction mechanism. *J Pept Sci.* 2012;18:541–8.
27. Pawar H, Douromumis D, Boateng JS. Preparation and optimization of PMAA-chitosan-PEG nanoparticle for oral drug delivery. *Coll Surf B.* 2012;90:102–8.
28. Saupe A, Gordon K, Rades T. Structural investigations on microemulsions, solid lipid nanoparticles, and nanostructured lipid carriers by cryo-field emission scanning electron microscopy, and Raman spectroscopy. *Int J Pharm.* 2006;314:56–62.
29. Ortiz C, Zhang DM, Xie Y, Davisson JV, Ben-Amotz D. Identification of insulin variants using Raman spectroscopy. *Anal Biochem.* 2004;332:245–52.
30. Tay SLM, Heng PWS, Chan LW. An investigation of the chick chorioallantoic membrane as an alternative model to various biological tissues for permeation studies. *J Pharm Pharmacol.* 2011;63:1283–9.
31. Haigh JM, Beyssac E, Chanet L, Aiache JM. In vitro permeation of progesterone from a gel through shed skin of three different snake species. *Int J Pharm.* 1998;170:151–6.